DYNAMIC PORTFOLIO CUTS: A SPECTRAL APPROACH TO GRAPH-THEORETIC DIVERSIFICATION

Alvaro Arroyo[1]*, Bruno Scalzo*[1]*, Ljubiša Stanković*[2]*, Danilo P. Mandic*[1]

[1]Department of EEE, Imperial College London, London, SW7 2BT, UK
[2]Faculty of Electrical Engineering, University of Montenegro, Podgorica, 81000, Montenegro
Emails: {alvaro.arroyo17, bruno.scalzo-dees12, d.mandic}@imperial.ac.uk, ljubisa@ucg.ac.me

ABSTRACT

Stock market returns are typically analyzed using standard regression models yet they reside on irregular domains, a natural scenario for *graph signal processing*. This motivates us to consider a *market graph* as an intuitive way to represent the relationships between financial assets. Traditional methods for estimating asset-return covariance operate under the assumption of statistical time-invariance, and are thus unable to appropriately infer the underlying structure of the market graph. To this end, this work introduces a class of graph spectral estimators which cater for the nonstationarity inherent to asset price movements, as a basis to represent the time-varying interactions between assets through a *dynamic spectral market graph*. Such an account of the time-varying nature of the asset-return covariance allows us to introduce the notion of *dynamic spectral portfolio cuts*, whereby the graph is partitioned into time-evolving clusters, thus allowing for robust and online asset allocation. The advantages of the proposed framework over traditional methods are demonstrated through numerical case studies using real-world price data.

Index Terms— Financial signal processing, portfolio optimization, spectral analysis, augmented complex statistics, nonstationarity, graph theory, graph cut, vertex clustering

1. INTRODUCTION

The asset-return covariance matrix is central to Modern Portfolio Theory (MPT), and underpins the mathematical analysis of financial markets [1][2][3][4]. Investment strategies typically consider a vector, $\mathbf{r}(t) \in \mathbb{R}^N$, which contains the returns of N assets at a time instant t, the i-th entry of which is given by [5]

$$r_i(t) = \frac{p_i(t) - p_i(t-1)}{p_i(t-1)} \tag{1}$$

where $p_i(t)$ denotes the value of the i-th asset at a time t. The mean-variance optimization of portfolios asserts that the optimal weighting vector of assets, $\mathbf{w} \in \mathbb{R}^N$, is obtained as

$$\min_{\mathbf{w}} \{\mathbf{w}^\mathsf{T}\mathbf{R}\mathbf{w}\} \quad \text{s.t.} \;\; \mathbf{w}^\mathsf{T}\mathbf{m} = \overline{\mu}; \;\; \mathbf{w}^\mathsf{T}\mathbf{1} = 1 \tag{2}$$

where $\mathbf{m} = E\{\mathbf{r}\} \in \mathbb{R}^N$ is a vector of expected future returns, $\mathbf{R} = \mathsf{cov}\{\mathbf{r}\} \in \mathbb{R}^{N\times N}$ is the covariance matrix of returns, $\overline{\mu}$ is the *expected return target*, and the second constraint, $\mathbf{w}^\mathsf{T}\mathbf{1} = 1$, guarantees full allocation of capital. Despite strong theoretical foundations behind MPT, one important unresolved issue remains an accurate estimation of matrix $\mathbf{R}$ [6][7][8], as well as instability issues associated with its inversion [9][10]. Recent work [11] proposes to resolve these issues through the *portfolio cut* paradigm, based on *vertex clustering* [12][13][14] of the *market graph* [15][16][17][18]. By segmenting the original market graph into computationally feasible and economically meaningful clusters of assets, schemes such as *hierarchical risk parity* [10] or *hierarchical clustering based asset allocation* [19] can be used to effectively allocate capital and generate wealth.

Despite their intuitive nature, the above approaches rest upon an unrealistic assumption of time-invariance of the covariance matrix, $\mathbf{R}$, despite the well established fact that financial markets follow nonstationary dynamics [20][21][22]. Furthermore, the use of sample estimators in nonstationary environments has been demonstrated to incur significant information loss, as established by von Neumann's *mean ergodic theorem* [23] and Koopman's *operator theory* [24]. This can be seen by considering an idealised case whereby the asset price returns evolve in time according to $\mathbf{r}(t) = \mathcal{S}\mathbf{r}(t-1)$, with $\mathcal{S} : \mathbb{C}^N \mapsto \mathbb{C}^N$ denoting a unitary *shift operator* in a Hilbert space. The mean ergodic theorem then asserts that the sample mean does approach the orthogonal subspace of $\mathbf{r}(t)$, that is

$$\lim_{T\to\infty} \frac{1}{T}\sum_{t=0}^{T-1} \mathbf{r}(t) = \lim_{T\to\infty} \frac{1}{T}\sum_{t=0}^{T-1} \mathcal{S}^t(\mathbf{r}(0)) = \mathcal{P}\mathbf{r}(0) \tag{3}$$

where $\mathcal{P}$ is the orthogonal projection onto the null space of $(\mathbf{I} - \mathcal{S})$, for which $\|\mathcal{P}\mathbf{r}(t)\|_2 \leq \|\mathbf{r}(t)\|_2$ holds owing to the Cauchy-Schwarz inequality.

In the context of graph data analytics, the need to account for the evolution of the underlying system dynamics has driven the development of dynamic learning systems [25], such as *temporal graph networks* [26]. We proceed a step further, and employ a recently proposed class of spectral estimators for nonstationary signals [27], to retrieve a time-varying covariance matrix, $\mathbf{R}(t)$, which caters for cyclostationary properties in market data. This serves as a basis to reformulate the definition of graph connectivity matrices of the market graph, in order to allow them to vary with time and account for long-term economic cycles present in the data. Such nonstationary graph signal processing [28] operators are shown to allow us to introduce the concept of *dynamic spectral vertex clustering* which serves as a basis for the proposed *dynamic spectral portfolio cut*. We demonstrate that this makes it possible to account for the seasonal correlations between vertices in the market graph, an important feature in the diversification of investment strategies which is completely overlooked by existing static graph topologies.

2. PRELIMINARIES

2.1. A Class of Nonstationary Signal Operators

Consider a time-frequency expansion [29][30] of the asset returns, $\mathbf{r}(t) \in \mathbb{R}^N$, given by

$$\mathbf{r}(t) = \int_{-\infty}^{\infty} e^{\jmath\omega t}\, \mathbb{r}(t,\omega)\, d\omega \tag{4}$$

where $\mathbb{r}(t,\omega) \in \mathbb{C}^N$ is the realisation of a random spectral process at an angular frequency, ω, at a time instant, t. The "augmented form" of this spectral process is then [31]

$$\underline{\mathbb{r}}(t,\omega) = \begin{bmatrix} \mathbb{r}(t,\omega) \\ \mathbb{r}^*(t,\omega) \end{bmatrix} \in \mathbb{C}^{2N} \tag{5}$$

The augmented spectral variable at each time instant is assumed to be *multivariate complex Gaussian distributed*, with its probability density function (pdf) is given by [27]

$$p(\underline{\mathbb{r}},t,\omega) = \frac{\exp\left[-\frac{1}{2}(\underline{\mathbb{r}}(t,\omega)-\underline{\mathbb{m}}(\omega))^{\mathsf{H}}\underline{\mathbb{R}}^{-1}(\omega)(\underline{\mathbb{r}}(t,\omega)-\underline{\mathbb{m}}(\omega))\right]}{\pi^N \det^{\frac{1}{2}}(\underline{\mathbb{R}}(\omega))} \tag{6}$$

where the *augmented* spectral mean and covariance are respectively given by [31]

$$\underline{\mathbb{m}}(\omega) = E\left\{\underline{\mathbb{x}}(t,\omega)\right\} = \begin{bmatrix} \mathbb{m}(\omega) \\ \mathbb{m}^*(\omega) \end{bmatrix} \tag{7}$$

$$\underline{\mathbb{R}}(\omega) = \mathsf{cov}\left\{\underline{\mathbb{x}}(t,\omega)\right\} = \begin{bmatrix} \mathbb{R}(\omega) & \mathbb{P}(\omega) \\ \mathbb{P}^*(\omega) & \mathbb{R}^*(\omega) \end{bmatrix} \tag{8}$$

Owing to the linearity of the Fourier operator, the time-domain counterpart of the spectral variable will also be multivariate Gaussian distributed, since a linear function of Gaussian random variables is also Gaussian distributed. Hence, the vector of returns, $\mathbf{r}(t)$, is distributed as

$$\mathbf{r}(t) \sim \mathcal{N}\left(\mathbf{m}(t), \mathbf{R}(t)\right) \tag{9}$$

where $\mathbf{m}(t) \in \mathbb{R}^N$ and $\mathbf{R}(t) \in \mathbb{R}^{N\times N}$ are respectively the time-varying mean vector and covariance matrix. Of particular interest to this work is the time-varying covariance, defined as [27]

$$\begin{aligned}\mathbf{R}(t) &= \mathsf{cov}\left\{\mathbf{r}(t)\right\} = E\left\{\mathbf{s}(t)\mathbf{s}^{\mathsf{T}}(t)\right\} \\ &= \int_{-\infty}^{\infty}\int_{-\infty}^{\infty} e^{\jmath(\omega-\nu)t}\mathbb{R}(\omega,\nu) + e^{\jmath(\omega+\nu)t}\mathbb{P}(\omega,\nu)\, d\omega d\nu \end{aligned} \tag{10}$$

where $\mathbf{s}(t) = \mathbf{r}(t) - \mathbf{m}(t)$ denotes the *centred* returns. Observe that $\mathbf{R}(t)$ represents a sum of *cyclostationary* components, each modulated at an angular frequency, ω.

2.2. Compact Spectral Representation

In order to discretize the above concept, consider a set of M frequency bins, $\boldsymbol{\omega} = [\omega_1, ..., \omega_M]^{\mathsf{T}}$, which form a discrete frequency spectrum, so that the time-frequency expansion in (4) therefore becomes

$$\mathbf{r}(t) = \frac{1}{\sqrt{2M}}\sum_{m=1}^{M}\left(e^{\jmath\omega_m t}\mathbb{r}(t,\omega_m) + e^{-\jmath\omega_m t}\mathbb{r}^*(t,\omega_m)\right) \tag{11}$$

or in a compact form

$$\mathbf{r}(t) = \underline{\boldsymbol{\Phi}}(t,\boldsymbol{\omega})\underline{\mathbb{r}}(t,\boldsymbol{\omega}) \tag{12}$$

The term $\underline{\boldsymbol{\Phi}}(t,\boldsymbol{\omega}) \in \mathbb{C}^{N\times 2MN}$ is referred to as the *augmented spectral basis*, and is defined as

$$\underline{\boldsymbol{\Phi}}(t,\boldsymbol{\omega}) = \begin{bmatrix} \boldsymbol{\Phi}(t,\boldsymbol{\omega}) & \boldsymbol{\Phi}^*(t,\boldsymbol{\omega}) \end{bmatrix} \tag{13}$$

$$\boldsymbol{\Phi}(t,\boldsymbol{\omega}) = \frac{1}{\sqrt{2M}}\begin{bmatrix} e^{\jmath\omega_1 t}\mathbf{I}_N & \cdots & e^{\jmath\omega_M t}\mathbf{I}_N \end{bmatrix} \tag{14}$$

with $\mathbf{I}_N \in \mathbb{R}^{N\times N}$ as the identity matrix, and $\underline{\mathbb{r}}(t,\boldsymbol{\omega}) \in \mathbb{C}^{2MN}$ as the *augmented spectrum representation*, given by

$$\underline{\mathbb{r}}(t,\boldsymbol{\omega}) = \begin{bmatrix} \mathbb{r}(t,\boldsymbol{\omega}) \\ \mathbb{r}^*(t,\boldsymbol{\omega}) \end{bmatrix}, \quad \mathbb{r}(t,\boldsymbol{\omega}) = \begin{bmatrix} \mathbb{r}(t,\omega_1) \\ \vdots \\ \mathbb{r}(t,\omega_M) \end{bmatrix} \tag{15}$$

Similarly, the *augmented spectral mean*, $\underline{\mathbb{m}}(\boldsymbol{\omega}) \in \mathbb{C}^{2MN}$, defined as

$$\underline{\mathbb{m}}(\boldsymbol{\omega}) = E\left\{\underline{\mathbb{r}}(t,\boldsymbol{\omega})\right\} = \begin{bmatrix} \mathbb{m}(\boldsymbol{\omega}) \\ \mathbb{m}^*(\boldsymbol{\omega}) \end{bmatrix}, \quad \mathbb{m}(\boldsymbol{\omega}) = \begin{bmatrix} \mathbb{m}(\omega_1) \\ \vdots \\ \mathbb{m}(\omega_N) \end{bmatrix} \tag{16}$$

follows the augmented complex form [31], while the *augmented spectral covariance*, $\underline{\mathbb{R}}(\boldsymbol{\omega}) \in \mathbb{C}^{2MN\times 2MN}$, is given by

$$\begin{aligned}\underline{\mathbb{R}}(\boldsymbol{\omega}) &= \mathsf{cov}\left\{\underline{\mathbb{r}}(t,\boldsymbol{\omega})\right\} = \begin{bmatrix} \mathbb{R}(\boldsymbol{\omega}) & \mathbb{P}(\boldsymbol{\omega}) \\ \mathbb{P}^*(\boldsymbol{\omega}) & \mathbb{R}^*(\boldsymbol{\omega}) \end{bmatrix} \\ \mathbb{R}(\boldsymbol{\omega}) &= \begin{bmatrix} \mathbb{R}(\omega_1) & \cdots & \mathbb{R}(\omega_1,\omega_M) \\ \vdots & \ddots & \vdots \\ \mathbb{R}(\omega_M,\omega_1) & \cdots & \mathbb{R}(\omega_M) \end{bmatrix} \\ \mathbb{P}(\boldsymbol{\omega}) &= \begin{bmatrix} \mathbb{P}(\omega_1) & \cdots & \mathbb{P}(\omega_1,\omega_M) \\ \vdots & \ddots & \vdots \\ \mathbb{P}(\omega_M,\omega_1) & \cdots & \mathbb{P}(\omega_M) \end{bmatrix} \end{aligned} \tag{17}$$

Finally, we arrive at the least-squares estimates of the augmented spectral moments [27], in the form

$$\hat{\underline{\mathbb{m}}}(\boldsymbol{\omega}) = \frac{1}{T}\sum_{t=0}^{T-1}\underline{\boldsymbol{\Phi}}^{\mathsf{H}}(t,\boldsymbol{\omega})\mathbf{r}(t) \tag{18}$$

$$\hat{\underline{\mathbb{R}}}(\boldsymbol{\omega}) = \frac{1}{T}\sum_{t=0}^{T-1}\underline{\boldsymbol{\Phi}}^{\mathsf{H}}(t,\boldsymbol{\omega})\hat{\mathbf{s}}(t)\hat{\mathbf{s}}^{\mathsf{T}}(t)\underline{\boldsymbol{\Phi}}(t,\boldsymbol{\omega}) \tag{19}$$

with $\hat{\mathbf{s}}(t) = \mathbf{r}(t) - \hat{\mathbf{m}}(t) = \mathbf{r}(t) - \underline{\boldsymbol{\Phi}}(t,\boldsymbol{\omega})\hat{\underline{\mathbb{m}}}(\boldsymbol{\omega})$.

2.3. Graph-Theoretic Diversification

2.3.1. Graph Signal Processing

Following the notation in [12], we define a graph $\mathcal{G} = \{\mathcal{V}, \mathcal{B}\}$ as being composed of a set of vertices $\mathcal{V}$, which are connected through a set of edges, $\mathcal{B} \subset \mathcal{V}\times\mathcal{V}$, where the symbol $\times$ denotes a direct product operator.

The connectivity of a graph, $\mathcal{G}$, is described through a *weight matrix*, $\mathbf{W} \in \mathbb{R}^{N\times N}$, the elements of which are non-negative real numbers, which designate the connection strength between the vertices m and n, so that

$$W_{mn}\begin{cases} > 0 & \text{if } (m,n) \in \mathcal{B} \\ = 0 & \text{if } (m,n) \notin \mathcal{B} \end{cases} \tag{20}$$

The *degree matrix*, $\mathbf{D} \in \mathbb{R}^{N\times N}$, is a diagonal matrix whose diagonal elements, D_{nn}, are equal to the sum of weights of all edges connected to a vertex n in an undirected graph, that is

$$D_{nn} = \sum_{m=1}^{N} W_{nm} \tag{21}$$

while the *graph Laplacian matrix* is given by

$$\mathbf{L} = \mathbf{D} - \mathbf{W} \tag{22}$$

2.3.2. Market Graph

A universe of N assets can be modeled as a *market graph*, with the weight matrix defined as

$$\mathbf{W} = \begin{bmatrix} 0 & \frac{|\sigma_{12}|}{\sqrt{\sigma_{11}\sigma_{22}}} & \cdots & \frac{|\sigma_{1N}|}{\sqrt{\sigma_{11}\sigma_{NN}}} \\ \frac{|\sigma_{21}|}{\sqrt{\sigma_{11}\sigma_{22}}} & 0 & \cdots & \frac{|\sigma_{2N}|}{\sqrt{\sigma_{22}\sigma_{NN}}} \\ \vdots & \vdots & \ddots & \vdots \\ \frac{|\sigma_{N1}|}{\sqrt{\sigma_{NN}\sigma_{11}}} & \frac{|\sigma_{N2}|}{\sqrt{\sigma_{NN}\sigma_{22}}} & \cdots & 0 \end{bmatrix} \tag{23}$$

where σ_{nm} denotes the covariance between the returns of asset n and asset m. Note the symmetry property of the weight matrix, that is, $\sigma_{nm} = \sigma_{mn}$.

Remark 1. The diagonal of the weight matrix is imposed to be zero, in order to prevent non-informative self-connections in the graph.

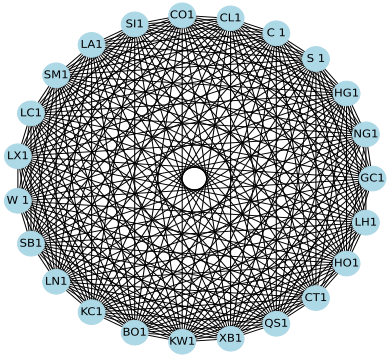

Fig. 1: Market graph formed from the 23 assets in the *Bloomberg Commodity Index*.

Remark 2. Fig. 1 illustrates one of the fundamental problems when using the covariance matrix in the context of financial investment, as it assumes full vertex connectivity, and thus does not appropriately account for real-world market structure [10][11][32][33].

2.3.3. Vertex Clustering and Minimum Cuts

In order to allow for the clustering of asset vertices into distinct sub-groups, we shall introduce vertex clustering based on *minimum cuts*.

Given an undirected graph, $\mathcal{G}$, defined by a set of vertices, $\mathcal{V}$, and edge weights, $\mathcal{W}$, we desire to group the vertices of the graph into two subsets, $\mathcal{E}$ and $\mathcal{H}$, such that $\mathcal{E} \subset \mathcal{V}$, $\mathcal{H} \subset \mathcal{V}$, $\mathcal{E} \cup \mathcal{H} = \mathcal{V}$ and $\mathcal{E} \cap \mathcal{H} = \emptyset$. To this end, a cut of graph, $\mathcal{G}$, given the subset of vertices $\mathcal{E}$ and $\mathcal{H}$, is given by [12]

$$Cut(\mathcal{E}, \mathcal{H}) = \sum_{m \in \mathcal{E}, n \in \mathcal{H}} W_{mn} \tag{24}$$

A *minimum cut* is then the cut which exhibits the minimal sum of weights joining subsets $\mathcal{E}$ and $\mathcal{B}$. Note that finding the minimal cut in a graph is a combinatorial problem, and thus computationally prohibitive for large graph topologies.

In the context of asset allocation in portfolios, it is often desirable that sub-graphs are as a large as possible, to prevent large disparity in asset splits. This motivates the definition of a *normalised ratio cut*, which takes the form [34]

$$CutN(\mathcal{E}, \mathcal{H}) = \left(\frac{1}{N_{\mathcal{E}}} + \frac{1}{N_{\mathcal{H}}}\right) \sum_{m \in \mathcal{E}, n \in \mathcal{H}} W_{mn} \tag{25}$$

where $N_{\mathcal{E}}$ and $N_{\mathcal{H}}$ represent the number of elements in the subsets $\mathcal{E}$ and $\mathcal{H}$, respectively. The first step to obtaining a computationally tractable way of performing minimum-cut-based vertex clustering is through the notion of of an *indicator vector*, $\mathbf{x} \in \mathbb{R}^N$. The elements of an indicator vector are *sub-graph-wise constant*, with the constant values within each cluster of vertices, but with distinct values across the clusters. This implies that the indicator may serve to uniquely identify the assumed cut of the graph into disjoint subsets [11], as *e.g.* in the case of two sub-graphs [12]

$$x(n) = \begin{cases} \frac{1}{N_{\mathcal{E}}}, & \text{if } n \in \mathcal{E} \\ -\frac{1}{N_{\mathcal{H}}}, & \text{if } n \in \mathcal{H} \end{cases} \tag{26}$$

The normalized cut defined in (25), can be written in terms of the graph Laplacian, $\mathbf{L}$, and indicator vector, $\mathbf{x}$, as

$$CutN(\mathcal{E}, \mathcal{H}) = \frac{\mathbf{x}^{\mathrm{T}}\mathbf{L}\mathbf{x}}{\mathbf{x}^{\mathrm{T}}\mathbf{x}} \tag{27}$$

so that the normalized cut can be considered as a minimization problem of the form

$$\min_{\mathbf{x}} \ \mathbf{x}^{\mathrm{T}}\mathbf{L}\mathbf{x}; \ \text{ s.t. } \ \mathbf{x}^{\mathrm{T}}\mathbf{x} = 1, \text{ and } \ \mathbf{x}^{T}\mathbf{1} = 0 \tag{28}$$

The solution to the above problem is given by $\mathbf{x}_{\text{opt}} = \mathbf{u}_1$ [12], that is, the second eigenvector of the graph Laplacian, $\mathbf{L}$, also known as the *Fiedler* eigenvector [35]. Furthermore, membership of a vertex to each subset is uniquely determined by the sign of $\mathbf{x}_{\text{opt}}$ [12].

Remark 3. Note that the second constraint in the optimization problem avoids the trivial solution $\mathbf{x}_{\text{opt}} = \mathbf{u}_0$, which is a constant eigenvector.

3. DYNAMIC SPECTRAL PORTFOLIO CUTS

Based on the above graph-theoretic interpretation of financial markets, we proceed to introduce a *dynamic market graph*, based on the time-varying covariance matrix presented in (10). To this end, we first define the *dynamic weight matrix* as

$$\mathbf{W}(t) = \mathbf{V}(t)\big|\mathbf{R}(t)\big|\mathbf{V}^{\mathrm{T}}(t) \tag{29}$$

where $\mathbf{V}(t)$ is a diagonal matrix containing the inverse square root of the diagonal elements in $\mathbf{R}(t)$ at a given time instant, t, in accordance with the definition in (23). Note that the modulus operator $|\cdot|$ is applied element-wise. This time-varying generalisation of the market graph makes it possible to capture economic cycles and shocks, thus allowing for a more meaningful and informative analysis of asset relationships.

In the context of graph data analytics, time-varying graph matrices naturally give rise to the concept of *dynamic graph matrix spectra*, whereby the eigenspectrum and eigenspace also become nonstationary, and contain the embedded information on the cyclical relationships captured by $\mathbf{R}(t)$. Mathematically, the singular value decomposition of the graph weight matrix in (29) now becomes

$$\mathbf{W}(t) = \mathbf{U}(t)\mathbf{\Lambda}(t)\mathbf{U}^{\mathrm{T}}(t) \tag{30}$$

given that $\mathbf{W}(t)$ it is a symmetric square invertible matrix. The eigenvector and eigenvalue matrices, $\mathbf{U}(t)$ and $\mathbf{\Lambda}(t)$, are in turn respectively given by

$$\mathbf{U}(t) = \begin{bmatrix} \mathbf{u}_1(t) & \mathbf{u}_2(t) & \dots & \mathbf{u}_N(t) \end{bmatrix} \tag{31}$$

$$\mathbf{\Lambda}(t) = \begin{bmatrix} \lambda_1(t) & 0 & \dots & 0 \\ 0 & \lambda_2(t) & \dots & 0 \\ \vdots & \vdots & \ddots & \vdots \\ 0 & 0 & \dots & \lambda_N(t) \end{bmatrix} \tag{32}$$

This allows us to introduce a time-varying extention of the operations traditionally performed on graphs, which we refer to as *dynamic graph data analytics*, which includes the notions of time-varying clustering and vertex dimensionality reduction. In the context of the market graph, this would imply the clustering of assets into different sub-graphs at each time instant, t, thereby enabling a more accurate modelling of the seasonal economical relationships between assets across a business year.

Following the capital allocation scheme proposed in [11], we denote by w_i the percentage of capital allocated to a market sub-graph $\mathcal{G}_i$, and consider two cases:

1. $w_i = \frac{1}{2^{K_i}}$, where K_i represents the number of cuts made to the market graph to obtain the cluster in question;
2. $w_i = \frac{1}{K+1}$, where K represents the number of individual clusters generated through the cuts.

This enables the formation of a portfolio at each time-instant, t, based on the estimated market graph topology at that moment.

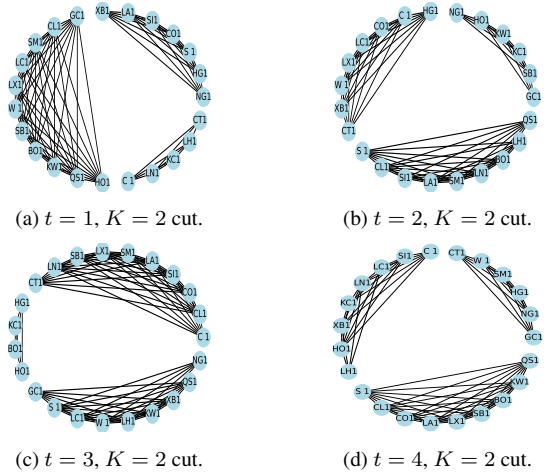

(a) $t = 1$, $K = 2$ cut. (b) $t = 2$, $K = 2$ cut.

(c) $t = 3$, $K = 2$ cut. (d) $t = 4$, $K = 2$ cut.

Fig. 2: Example of $K = 2$ minimum cuts performed on the the *Bloomberg Commodity Index* (BCOM) market graph over four time-steps. Different cluster formations are generated at each time-instant, owing to the dynamic nature of the graph weight matrix.

4. SIMULATIONS

The performance of the proposed dynamic portfolio cuts framework was investigated using historical daily price data of the 23 commodity futures contracts constituting the Bloomberg Commodity Index in the period 2010-01-01 to 2021-05-17, as well as the 100 most liquid stocks in the S&P 500 index, based on the average trading volume, between 2015-01-01 to 2021-05-17. The data was partitioned into a *training* (in-sample) dataset, from 2010-01-01 to 2016-01-01 for the BCOM index and 2014-01-02 to 2020-01-02 for the S&P 500, which was used to estimate the spectral covariance and retrieve its time-varying counterpart. Subsequently, asset clustering was carried out on the dynamic market graph and tested on data from the *test* (out-of-sample) dataset, with the dates 2016-01-01 to 2021-05-17 for the BCOM index and 2020-01-02 to 2021-05-17 for the S&P 500. Fig. 3 shows a comparison between the proposed dynamic portfolio cut and its static counterpart, as well as standard equally-weighted (EW) and MV (mean-variance optimized) portfolios.

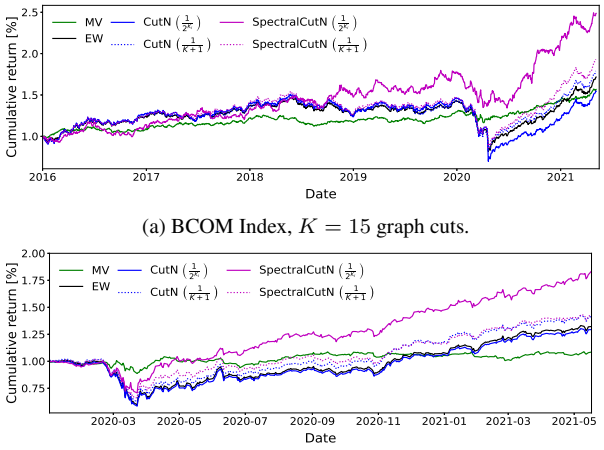

(a) BCOM Index, $K = 15$ graph cuts.

(b) S&P 500 Index, $K = 10$ graph cuts.

Fig. 3: Out-of-sample performance of all strategies.

Fig. 3 shows that the proposed dynamic spectral cuts framework consistently yields a larger cumulative return compared to both standard and existing graph-based approaches. As desired, the so enabled high average returns, coupled with the low variance of the proposed strategy, result in higher *Sharpe ratios* (*i.e.* the ratio of the mean to the standard deviation of portfolio returns) as summarized in Tables 1 and 2.

Table 1: Sharpe ratio for varying number of cuts K in BCOM Index.

Strategy	Allocation	$K=1$	$K=2$	$K=3$	$K=4$	$K=5$	$K=10$	$K=15$
SpectralCutN	$\frac{1}{2^{K_i}}$	**2.15**	2.77	**2.7**	**2.73**	**2.72**	**2.89**	**3.19**
SpectralCutN	$\frac{1}{K+1}$	**2.15**	**2.88**	2.51	2.37	1.75	2.22	1.71
CutN	$\frac{1}{2^{K_i}}$	1.96	1.14	1.12	2.22	2.08	0.75	1.07
CutN	$\frac{1}{K+1}$	1.62	1.81	1.86	1.85	1.99	1.78	1.3

Table 2: Sharpe ratio for varying number of cuts K in S&P 500.

Strategy	Allocation	$K=1$	$K=2$	$K=3$	$K=4$	$K=5$	$K=10$	$K=50$
SpectralCutN	$\frac{1}{2^{K_i}}$	1.61	**1.78**	**1.86**	**1.87**	**1.87**	**1.88**	**1.76**
SpectralCutN	$\frac{1}{K+1}$	1.61	1.6	1.51	1.37	1.21	1.12	0.97
CutN	$\frac{1}{2^{K_i}}$	0.86	0.81	0.94	0.86	0.84	0.82	0.85
CutN	$\frac{1}{K+1}$	**1.63**	1.5	1.23	1.35	1.25	1.05	0.91

Remark 4. Note that graph-based portfolio strategies inevitably result in long-only portfolios, given the positive weights connecting the vertices of a graph. As such, portfolio cuts and dynamic portfolio cuts are expected to work well on upward trending indices, such as the S&P 500, which are only composed of stocks, and have a tendency to grow over time.

5. CONCLUSIONS

A novel dynamic spectral graph framework has been introduced which allows for real-time modelling of the interaction of financial assets residing on the market graph over time. This is achieved through a class of spectral estimators of the augmented spectral covariance, which is shown to account for cyclostationary trends in market data, and thus for economic cycles and shocks. Simulations have demonstrated the advantages of the proposed framework over stationary portfolio cut techniques on the market graph, as well as a dominant performance over traditional portfolio optimization approaches.

6. REFERENCES

[1] H. Markowitz, "Portfolio selection," *Journal of Finance*, vol. 7, no. 1, pp. 77–91, 1952.

[2] A. Akansu and M. U. Torun, *A Primer for Financial Engineering*. Academic Press, 2015.

[3] A. Akansu, S. R. Kulkarni, and D. M. Malioutov, *Financial Signal Processing and Machine Learning*. Wiley, 2016.

[4] X. Zhang and F. Wang, "Signal processing for finance, economics, and marketing: Concepts, framework, and big data applications," *IEEE Signal Processing Magazine*, vol. 34, no. 3, pp. 14–35, 2017.

[5] Y. Feng and D. P. Palomar, "A signal processing perspective on financial engineering," *Foundations and Trends® in Signal Processing*, vol. 9, no. 1–2, pp. 1–231, 2016.

[6] V. K. Chopra and W. T. Ziemba, "The effect of errors in means, variances, and covariances on optimal portfolio choice," *The Journal of Portfolio Management*, vol. 19, no. 2, pp. 6–11, 1993.

[7] F. Rubio, X. Mestre, and D. P. Palomar, "Performance analysis and optimal selection of large minimum variance portfolios under estimation risk," *IEEE Journal of Selected Topics in Signal Processing*, vol. 6, no. 4, pp. 337–350, 2012.

[8] S. Deshmukh and A. Dubey, "Improved covariance matrix estimation with an application in portfolio optimization," *IEEE Signal Processing Letters*, vol. 27, pp. 985–989, 2020.

[9] D. Bailey and M. Lopez de Prado, "Balanced baskets: A new approach to trading and hedging risks," *Journal of Investment Strategies*, vol. 1, no. 4, pp. 21–62, 2012.

[10] N. J. Calkin and M. Lopez de Prado, "Building diversified portfolios that outperform out of sample," *The Journal of Portfolio Management*, vol. 42, no. 4, pp. 59–69, 2016.

[11] B. Scalzo, A. G. Constantinides, and D. P. Mandic, "Portfolio cuts: A graph-theoretic framework to diversification," *In Proceedings of the IEEE International Conference on Acoustics Speech and Signal Processing (ICASSP)*, pp. 8454–8458, 2020.

[12] L. Stankovic, D. P. Mandic, M. Dakovic, M. Brajovic, B. Scalzo, and T. Constantinides, "Data analytics on graphs. Part I: Graphs and spectra on graphs," *Foundations and Trends in Machine Learning*, vol. 13, no. 1, pp. 1–157, 2020.

[13] ——, "Data analytics on graphs. Part II: Signals on graphs," *Foundations and Trends in Machine Learning*, vol. 13, no. 2–3, pp. 158–331, 2020.

[14] ——, "Data analytics on graphs. Part III: Machine learning on graphs, from graph topology to applications," *Foundations and Trends in Machine Learning*, vol. 13, no. 4, pp. 332–530, 2020.

[15] V. Boginski, S. Butenko, and P. M. Pardalos, "On structural properties of the market graph," in *Innovations in Financial and Economic Networks*, A. Nagurney, Ed. Edward Elgar Publishers, 2003, pp. 29–45.

[16] J. V. de Miranda Cardoso, J. Ying, and D. P. Palomar, "Algorithms for learning graphs in financial markets," *arxiv.2012.15410*, 2020.

[17] X. Wan, J. Yang, S. Marinov, J.-P. Calliess, S. Zohren, and X. Dong, "Sentiment correlation in financial news networks and associated market movements," *Scientific reports*, vol. 11, no. 1, pp. 1–12, 2021.

[18] J.-P. Onnela, A. Chakraborti, K. Kaski, J. Kertesz, and A. Kanto, "Asset trees and asset graphs in financial markets," *Physica Scripta*, vol. 2003, no. T106, p. 48, 2003.

[19] T. Raffinot, "Hierarchical clustering-based asset allocation," *The Journal of Portfolio Management*, vol. 44, no. 2, pp. 89–99, 2017.

[20] R. Cont, "Empirical properties of asset returns: Stylized facts and statistical issues," *Quantitative Finance*, vol. 1, no. 2, pp. 223–236, 2001.

[21] S. K. Guharay, G. S. Thakur, F. J. Goodman, S. L. Rosen, and D. Houser, "Analysis of non-stationary dynamics in the financial system," *Economics Letters*, vol. 121, no. 3, pp. 454–457, 2013.

[22] F. Tobar and M. Orchard, "Study of financial systems volatility using suboptimal estimation algorithms," *Studies in Informatics and Control*, vol. 21, pp. 59–66, 2012.

[23] J. von Neumann, "Proof of the quasi-ergodic hypothesis," *Proceedings of the National Academy of Sciences of the United States of America*, vol. 18, pp. 70–82, 1932.

[24] B. O. Koopman, "Hamiltonian systems and transformation in Hilbert space," *Proceedings of the National Academy of Sciences of the United States of America (PNAS)*, vol. 17, no. 5, pp. 315–318, 1931.

[25] S. M. Kazemi, R. Goel, K. Jain, I. Kobyzev, A. Sethi, P. Forsyth, and P. Poupart, "Representation learning for dynamic graphs: A survey." *Journal of Machine Learning Research*, vol. 21, no. 70, pp. 1–73, 2020.

[26] E. Rossi, B. Chamberlain, F. Frasca, D. Eynard, F. Monti, and M. M. Bronstein, "Temporal graph networks for deep learning on dynamic graphs," *arxiv.2006.10637*, 2020.

[27] B. Scalzo, A. Arroyo, L. Stanković, and D. P. Mandic, "Nonstationary portfolios: Diversification in the spectral domain," *In Proceedings of the IEEE International Conference on Acoustics Speech and Signal Processing (ICASSP)*, pp. 5155–5159, 2021.

[28] A. Ortega, P. Frossard, J. Kovacevic, J. M. F. Moura, and P. Vandergheynst, "Graph signal processing: Overview, challenges, and applications," *In Proceedings of the IEEE*, vol. 106, no. 5, pp. 808–828, 2018.

[29] M. Loève, *Probability Theory*. Springer-Verlag, 1977.

[30] P. J. Schreier and L. L. Scharf, "Stochastic time-frequency analysis using the analytic signal: Why the complementary distribution matters," *IEEE Transactions on Signal Processing*, vol. 51, no. 12, pp. 3071–3079, 2003.

[31] D. P. Mandic and V. S. L. Goh, *Complex Valued Nonlinear Adaptive Filters: Noncircularity, Widely Linear and Neural Models*. Wiley, 2009.

[32] N. J. Calkin and M. Lopez de Prado, "Stochastic flow diagrams," *Algorithmic Finance*, vol. 3, no. 1–2, pp. 21–42, 2014.

[33] ——, "The topology of macro financial flows: An application of stochastic flow diagrams," *Algorithmic Finance*, vol. 3, no. 1, pp. 43–85, 2014.

[34] L. Hagen and A. B. Kahng, "New spectral methods for ratio cut partitioning and clustering," *IEEE Transactions on Computer-Aided Design of Integrated Circuits and Systems*, vol. 11, no. 9, pp. 1074–1085, 1992.

[35] M. Fiedler, "Algebraic connectivity of graphs," *Czechoslovak Mathematical Journal*, vol. 23, no. 2, pp. 298–305, 1973.